Journal of Hazardous Materials 181 (2010) 736–741

Contents lists available at ScienceDirect

Journal of Hazardous Materials

journal homepage: www.elsevier.com/locate/jhazmat

Pyridine and phenol removal using natural and synthetic apatites as low cost sorbents: Influence of porosity and surface interactions

H.Bouyarmane[a], S.El Asri[a], A. Rami[b], C. Roux[c], M.A. Mahly[b], A. Saoiabi[a], T. Coradin[c,*], A. Laghzizil[a,*]

[a] Laboratoire de Chimie Physique Générale, Université Mohamed V, Faculté des Sciences BP.1014 Rabat, Morocco
[b] Laboratoire National de Contrôle des Médicaments, Rabat, Morocco
[c] UPMC-P6; CNRS, Chimie de la Matière Condensée de Paris, Collège de France, 75005 Paris, France

ARTICLE INFO

Article history:
Received 25 March 2010
Received in revised form 4 May 2010
Accepted 14 May 2010
Available online 8 June 2010

Keywords:
Pyridine
Phenol
Phosphate rock
Apatite
Remediation

ABSTRACT

A natural phosphate rock and two synthetic mesoporous hydroxyapatites were evaluated for the removal of pyridine and phenol from aqueous solutions. Experiments performed by the batch method showed that the sorption process occurs by a first order reaction for both pyridine and phenol. In contrast, the Freundlich model was able to describe sorption isotherms for phenol but not for pyridine. In parallel, the three apatites exhibit similar pyridine sorption capacities whereas phenol loading was in agreement with their respective specific surface area. This was attributed to the strong interaction arising between pyridine and apatite surface that hinders further inter-particular diffusion. This study suggests that, despite its low specific surface area, natural phosphate rock may be used as an efficient sorbent material for specific organic pollutants, with comparable efficiency and lower processing costs than some activated carbons.

1. Introduction

Pyridine and phenol are priority hazardous pollutants since they are toxic and harmful to organisms even at low concentration [1–3]. They are parents of series of compounds that are widely used as solvents and intermediates in the production of agricultural chemicals, dyestuffs and paints, polycarbonate resins and water-repellents textile, as well as in research laboratories. Pyridine is an N-heterocyclic aromatic compound with disagreeable odor, high water solubility and high volatility [4]. Both compounds are hazardous in nature and persist for long times in environment, as they are poor substrates to endogenous microorganisms [5]. The removal of toxic organic molecular species from wastewaters is therefore of great importance. Several methods are used for the removal of pyridine and phenol from water including biodegradation [5–7], adsorption (Rundle oil shale, clays, zeolites, granular activated carbon) [8–12], simultaneous adsorption and electrosorption [13], ozonation [14], and ion exchange [15–16]. Chemical oxidation and biodegradation methods are available for the treatment of wastes containing pyridine and phenol, but usually generate some toxic metabolites. Biological methods can provide a better option when using bioreactors for the treatment of gaseous emissions containing pyridine. In parallel, adsorption processes are often used at industrial scale for the removal of several pollutants using low-cost raw materials, due to their relative simplicity. In this context, hydroxyapatite exhibits good cation-exchange properties due to Ca^{2+} lability, favoring metal ion sorption [17–18]. Moreover, recent reports suggest that hydroxyapatite surfaces show a good affinity for organic pollutants [19–21]. In this case, mesoporous materials are highly desirable as they exhibit large specific surface area and suitable pore size.

With the aim of extending the range of applications of hydroxyapatite as an organic pollutant remediation material, we decided to investigate pyridine sorption on several apatite sorbents. With this purpose, a natural phosphate rock and two synthetic mesoporous apatites were selected. The sorption of phenol on the three materials was also studied. Noticeably, pyridine is traditionally used a probe for acidic surface studies whereas phenol is a model compound to investigate hydrogen bond formation so that the comparison between these two molecules was expected to provide further insights on the apatite surface reactivity. Kinetics and isotherm modeling was performed using Langergren and Langmuir-Freundlich models, respectively. Based on these data, it was possible to discuss the relative contribution of sorbent struc-

* Corresponding author. Tel.: +212537775440; fax: +212 537775440.
E-mail addresses: thibaud.coradin@upmc.fr (T. Coradin), laghzizi@fsr.ac.ma (A. Laghzizil).

0304-3894/$ – see front matter © 2010 Elsevier B.V. All rights reserved.
doi:10.1016/j.jhazmat.2010.05.074

Table 1
Chemical and textural characteristics (specific surface area S_{BET} and average pore size D_p) of three adsorbents [22–24].

Samples	Ca/P	Crystallinity	S_{BET} (m^2g^{-1})	D_p (nm)
PR	1.97	Good	20	20
c-HAp	1.95	Poor	150	10
p-HAp	1.61	Poor	230	10

ture and sorbent-pollutant interactions on the efficiency of the removal process.

2. Experimental

2.1. Adsorbents

Three apatite $Ca_{10}(PO_4)_6(OH)_2$ adsorbents were used in this study: phosphate rock (noted PR), converted mesoporous apatite from PR (noted c-HAp) and porous hydroxyapatite (p-HAp). The phosphate rock sample used in this work was from the Bengurir region (Morocco). The sample was washed and then sieved to give a 100-400 μm size fraction using ASTM Standard sieves. Previous analyses have shown that PR is a carbonaceous fluoroapatite containing *ca.* 4% quartz and *ca.* 7 wt% organics [22]. c-HAp was synthesized from phosphate rock by a dissolution–precipitation method recently described that provides a simple and economic route for synthesis of mesoporous apatite powders [23]. p-HAp was obtained by a chemical neutralization method from $Ca(OH)_2$ and $NH_4H_2PO_4$ as described elsewhere [24–25]. The main chemical and structural characteristics of the three materials have been gathered in Table 1. Pyridine (C_6H_5N) and phenol (C_6H_5-OH) (Sigma-Aldrich) were used as received.

2.2. Adsorption procedure

Sorption studies were performed by the batch technique due to its simplicity in order to obtain rate and equilibrium data at room temperature. For isotherm studies, a series of 100 cm^3 of aqueous solutions of each sorbate at concentrations 5–200 $mgdm^{-3}$ were used and adjusted to the desired pH at room temperature using diluted HCl or NaOH solutions. The selected adsorbent was then added at a fixed dose (2 gdm^{-3}). The pH was followed during the course of the reactions using a glass electrode with experimental variations in a 5% range. The used concentration range was chosen based on several preliminary investigations and in accordance with the levels of these hazardous species generally present in wastewater/industrial effluents. The contact time and other conditions were selected on the basis of the results of preliminary experiments. After the corresponding time interval, the suspensions were sampled through direct filtration using 0.45 μm membrane filter. The sorbate concentration in the supernatant was monitored using a UV-visible spectrophotometer (Perking Elmer Lamda II) working at λ = 255 nm and 274 nm for pyridine and phenol, respectively. All experiments were performed in triplicate and experimental errors were found below 5%. The sorbate concentration retained by the adsorbent surface was calculated by using Eq. (1):

$$q_t = \frac{C_0 - C(t)}{m}.V \quad (1)$$

where q_t is the amount (mgg^{-1}) of adsorbed organic molecules at time t, C_0 and $C(t)$ are their concentrations ($mgdm^{-3}$) in solution at t = 0 and t = t, V is the volume (dm^3) of contaminated solution and m is the mass (g) of the adsorbent.

2.3. Kinetics of pyridine sorption

Kinetics of pyridine and phenol adsorption on phosphate PR, c-HAp and p-HAp were determined in batch experiments at room temperature. 200 mg of adsorbent was held in contact with 100 cm^3 of solution containing 20 $mgdm^{-3}$ of pyridine or phenol. In order to determine the rate constants, the two most widely-used kinetic models in sorption processes (pseudo-first and pseudo-second order models) have been applied to experimental data. The Lagergren pseudo-first order equation can be expressed as [26]:

$$\log(q_e - q_t) = \log q_{e,1} - \frac{k_1}{2.303}t \quad (2)$$

where q_e are the amount (mgg^{-1}) of adsorbed organic molecules at equilibrium and k_1 a kinetic rate constant. This model can be applied if $log(q_e\text{-}q_t)$ versus t gives a straight line, in which case $q_{e,1}$ and k_1 can be calculated from the intercept and slope of the plot.

The pseudo-second order model can be expressed as a differential equation [27]:

$$\frac{t}{q_t} = \frac{1}{k_2 q_{e,2}^2} + \frac{1}{q_{e,2}}t \quad (3)$$

The plot of t/q_t against time t of Eq. (3) should give a linear relationship from which the constants $q_{e,2}$ and k_2 can be determined from the intercept and slope of the plot.

2.4. Modeling of the adsorption isotherms

The sorption isotherms are usually fitted using a simple Langmuir equation. However, surface heterogeneity may lead to significant deviation from experimental data and several empirical fitting equations have been developed, in particular the Freundlich model and its extension [28]:

$$\frac{q_e}{q_{e,\max}} = \frac{\alpha.C_0^{\beta}}{1 + \alpha.C_0^{\beta}} \quad (4)$$

with q_e the amount of adsorbed phenol or pyridine at equilibrium for an initial concentration C_0 and $q_{e,max} = q_e$ when $C_0 \to \infty$ (*i.e.* adsorption capacity). α and β are two constants related to the adsorbent-adsorbate interactions, although their precise physical meaning is still under study [29].

3. Results

3.1. Pyridine sorption

Fig. 1 shows the evolution of pyridine sorption onto phosphate rock PR, converted apatite c-HAp and synthetic hydroxyapatite p-HAp as a function of time for a 20 $mgdm^{-3}$ as initial sorbate concentration and a 2 gdm^{-3} of apatite content with an initial pH adjusted to 6. It can be observed that the maximum uptake of pyridine is reached after approximately 4 hours for the three adsorbents. In order to analyze the adsorption kinetics of pyridine, correlations between adsorbed amount and time were looked for. Table 2 gathers the parameters derived from the application of the Langergren pseudo first-order equation ($q_{e,1}$ and k_1) and the pseudo second-order kinetic model (k_2 and $q_{e,2}$). For the three sorbents, the corresponding correlation coefficients R^2 were generally below 0.99 but the most satisfactory fitting was obtained with the pseudo first-order equation. For this model, the calculated equilibrium sorption capacities were 8.7 mgg^{-1}, 8.3 mgg^{-1} and 8.9 mgg^{-1} for PR, c-HAp and p-HAp respectively, while the values of the rate constant, k_1, were found 0.005 min^{-1}, 0.011 min^{-1} and 0.007 min^{-1}, respectively, suggesting that the three materials exhibit nearby uptake kinetics. Therefore, the pseudo-first order

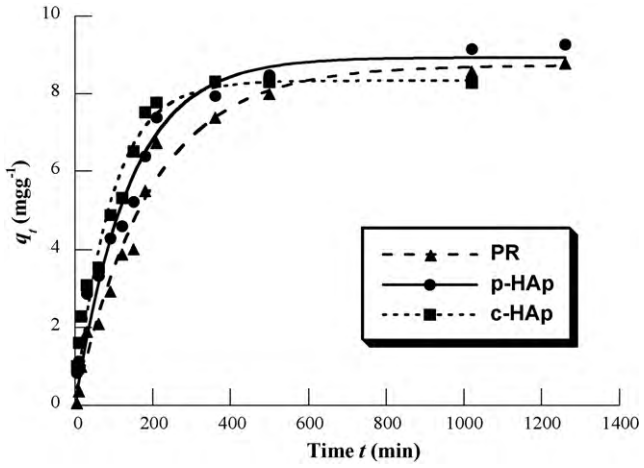

Fig. 1. Effect of contact time on the adsorption of pyridine on the three apatites. Lines indicate the result of modeling using the pseudo-first order equation.

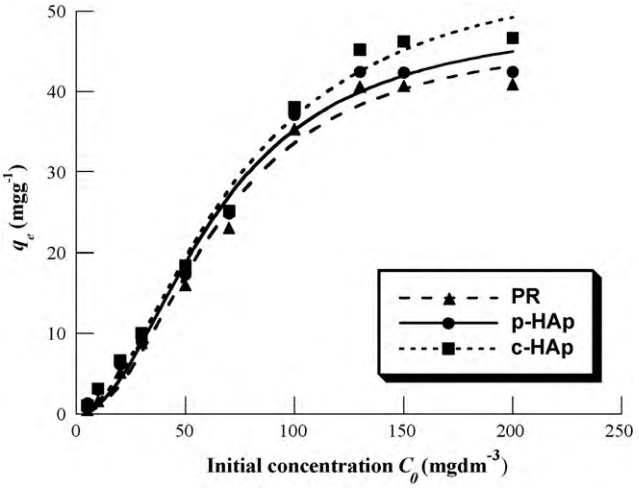

Fig. 2. Effect of initial concentration of pyridine on its adsorption on the three apatites. Lines indicate the result of modeling using the Freundlich equation.

Table 2
Kinetic rate constants (k) and adsorption capacities (q) as obtained for different models for pyridine and phenol sorption by mineral and synthetic apatites. R^2 indicates the correlation coefficients for the linear fits.

	Model	Parameter	PR	c-HAp	p-HAp
Pyridine	Pseudo first order	k_1 (min^{-1})	0.005	0.011	0.007
		$q_{e,1}$ (mgg^{-1})	8.7	8.3	8.9
		R^2	0.991	0.989	0.987
	Pseudo second order	k_2 (min^{-1})	0.002	0.004	0.004
		$q_{e,2}$ (gmg^{-1}min^{-1})	6.7	7.0	6.2
		R^2	0.953	0.965	0.988
Phenol	Pseudo first order	k_1 (min^{-1})	0.080	0.028	0.027
		$q_{e,1}$ (mgg^{-1})	1.7	3.1	5.5
		R^2	0.993	0.998	0.999
	Pseudo second order	k_2 (min^{-1})	0.088	0.093	0.011
		$q_{e,2}$ (gmg^{-1}min^{-1})	1.8	3.6	7.6
		R^2	0.998	0.995	0.956

model does show a good compliance with experimental data, as shown in Fig. 1. The pseudo second-order modeling gives sorption capacities, $q_{e,2}$ significantly lower than experimental data while the rate constants, k_2 differ significantly for the three materials, in contradiction with experimental data.

Sorption isotherms as a function of the initial pyridine concentration were obtained after 4 hours as contact time at the same initial pH (Fig. 2). The PR, c-HAp and p-HAp adsorbents show comparable experimental pyridine adsorption performances (46.8 mgg^{-1} for c-HAp compared to 40.2 mgg^{-1} for PR and 42.5 mgg^{-1} for p-HAp (Table 3). Attempts to use the Langmuir model for isotherm modeling were unsuccessful, as it was not suitable to reproduce the low concentration domain. In the case of the Freundlich equation, an apparently correct fitting of the experimental data was obtained ($R^2 > 0.99$), especially in the low concentration range. However, calculated maximum sorption capacities were higher than experimental values for PR and p-HAp and α values negligible (Table 3). Overall, it can be suggested that the pyridine sorption process is a complex, probably multi-step reaction that cannot be described by simple Langmuir and Freundlich models.

To get additional information on the adsorption mechanism, the evolution of the pH of the pyridine solution during sorption was measured (Fig. 3). In the absence of pyridine, the equilibrium pH equals 8.8 for PR and p-HAp and 7.9 for c-HAp. This corresponds to protonation of surface phosphate groups and, to a lesser extent, the release of alkaline species such as carbonates, during the equilibration between the apatite surface and water. In the presence of pyridine, the equilibrium pH is much more limited and stabilizes at 7.8 for PR and p-HAp and 6.8 for c-HAp. The influence of initial pH on pyridine sorption was also studied, showing that the amount of sorbed pyridine increases with pH up to pH 10 (Fig. 4).

3.2. Phenol sorption

Under the same conditions (pH = 6, sorbent dosage = 2 gdm^{-3}), in the presence of phenol, a maximum uptake is reached only after *ca.* 60 min and 120 min for PR and both c-HAp and p-HAp respectively, with a significant variation in sorbed amount as a function of the sorbent. (Fig. 5). When applying Lagergren pseudo first-order model, correlation coefficient $R^2 > 0.99$ were obtained and rate constants k were found to be 0.080 min^{-1}, 0.028 min^{-1} and 0.027 min^{-1} for PR, c-HAp and p-HAp respectively (Table 3). Calculated equilibrium sorption q_e values are 1.7 mgg^{-1} and 3.1 mgg^{-1} and 5.5 mgg^{-1} for PR, c-HAp and p-HAp respectively, in good agreement with experimental data, as shown on Fig. 5. Although reasonable correlation coefficients were obtained using the pseudo second-order model, an overestimation of the q_e value was obtained for the c-HAp (3.6 mgg^{-1}) and p-HAp (7.7 mgg^{-1}) samples.

Based on previous kinetics data, sorption isotherms were obtained after 3 hours of contact time, confirming that the three materials exhibit significantly different phenol sorption capacity (Fig. 6). Attempts to use the Langmuir model to analyze the experimental data were unsuccessful. In contrast, the Freundlich equation gives a very good agreement, with correlation coefficients $R^2 > 0.99$. Resulting calculated maximum sorption capacities were 5.0 mgg^{-1}, 7.2 mgg^{-1}, 8.4 mgg^{-1} for PR, c-HAp and p-HAp respectively. Therefore, phenol sorption occurs through a multilayer adsorption on the heterogeneous surface of apatite.

Table 3
Experimental sorption capacity ($q_{e,exp}$) and Freundlich parameters obtained from Freundlich modeling for the sorption of pyridine and phenol onto the three adsorbents.

		PR	c-HAp	p-HAp
Pyridine	$q_{e,exp}$ (mgg^{-1})	40.2	46.8	42.5
	$q_{e,max}$ (mgg^{-1})	43.9	45.6	51.6
	α	< 0.0001	< 0.0001	< 0.0001
	β	1.8	1.8	1.8
	R^2	0.994	0.994	0.995
Phenol	$q_{e,exp}$ (mgg^{-1})	3.9	6.5	8.2
	$q_{e,max}$ (mgg^{-1})	5.0	7.2	8.4
	α	0.006	0.009	0.066
	β	1.2	1.3	1.1
	R^2	0.996	0.997	0.998

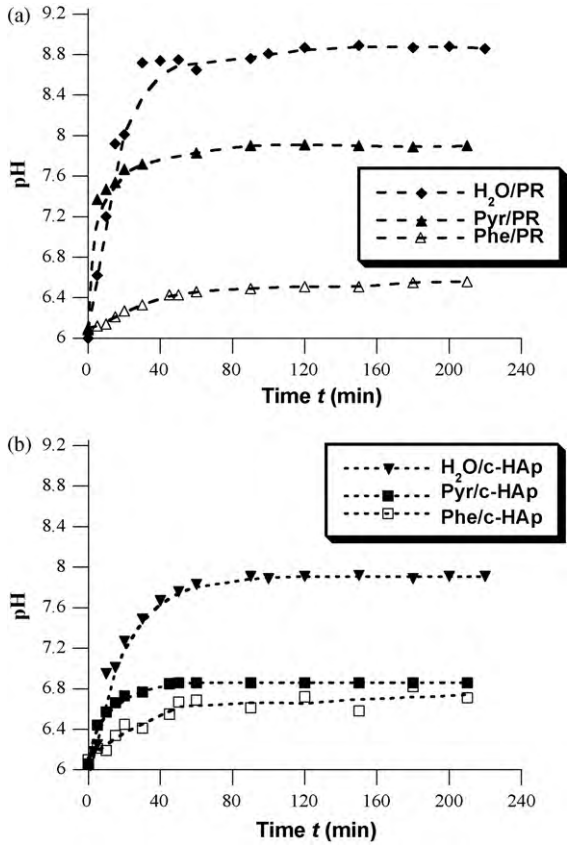

Fig. 3. Equilibrium pH change in the presence of (a) PR and (b) c-HAp with water (H_2O), with added pyridine (Pyr) or phenol (Phe). Data for p-HAp were similar to PR and are not shown for sake of clarity. Lines are provided as guidelines only.

The evolution of the pH of the phenol solution was also monitored during the sorption process (Fig. 3). In the presence of phenol, an increase of pH is observed with time but to a much lesser extent than for pyridine, especially for PR. The influence of pH on phenol adsorption was also studied (Fig. 4), showing that a maximum of adsorption is observed in acidic conditions, whereas a pH of minimum adsorption is observed in the 7-8 pH range.

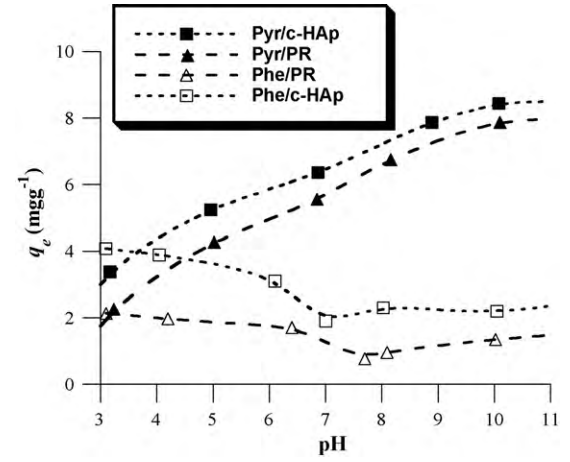

Fig. 4. Effect of initial pH on pyridine (Pyr) and phenol (Phe) adsorption by PR and c-HAp adsorbents. Data for p-HAp were similar to PR and are not shown for sake of clarity. Lines are provided as guidelines only.

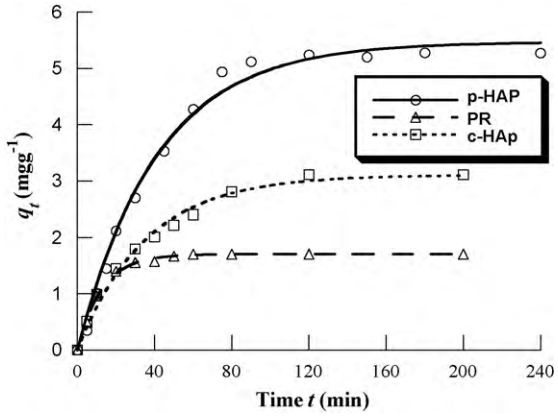

Fig. 5. Effect of contact time on the adsorption of phenol on the three apatites. Lines indicate the result of modeling using the pseudo-first order equation.

4. Discussion

This work represents the first evaluation of calcium phosphate materials for the removal of pyridine in aqueous solutions. Herepresented data indicate that the three, *i.e.* natural and synthetic, materials exhibit good pyridine sorption capacities. These capacities are comparable to activated carbons from cocunut shell and rubber seed coat ($q_{e,exp}$ = 20-100 mgg^{-1} compared to $q_{e,exp}$ = 40-46 mgg^{-1} in this study) [12,16]. However, the most surprising result of this study is that the natural phosphate PR and the porous synthetic hydroxyapatites (c-HAp and p-HAp) exhibit very similar pyridine sorption capacities, despite their highly different specific surface area. In comparison, significant differences in sorption capacity towards phenol are obtained, that correlate well with the evolution of the specific surface area of the three materials, *i.e.* p-HAp > c-HAp > PR. In the same time, the maximum sorption capacities, either experimental or calculated, are 5-7 times larger for the amine compared to the alcohol.

These sorption capacities can, in principle, be related to three main parameters: the accessible apatite surface, the molecular packing on the surface and the nature of the molecule-apatite interaction.

When considering the charge of the two organic species, pyridine and phenol have a pK_a of 5.20 and of 9.95, respectively. Therefore, at the beginning of the reaction (pH = 6), both molecules are in the neutral form. In the same conditions, the apatite surface charge is expected to result from the balance between P-OH, P-O$^-$

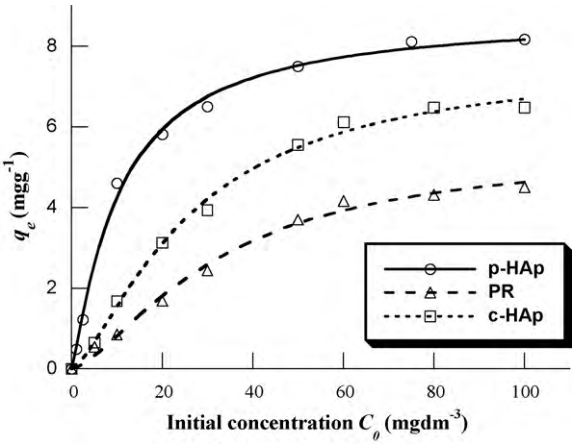

Fig. 6. Effect of initial concentration of phenol on its adsorption on the three apatites. Lines indicate the result of modeling using the Freundlich equation.

and Ca^{2+} groups. Therefore pyridine (or phenol) interactions with apatite surface are expected to be two-fold: hydrogen bonding with P-OH/P-O^- groups and Lewis acid-base interactions involving Ca^{2+} ions [30]. The latter is expected to be particularly efficient for pyridine bearing a lone free pair of electrons and the former for phenol due to its aromatic acidic hydroxyl group. As sorption proceeds, an increase in pH is observed but to a more limited extent than for apatite in pure water. These observations may result from two effects related to phosphate groups reactivity: first, the sorption of phenol by P-$O^-\cdots$HO-C_6H_5 hydrogen bond; second, the sorption of pyridine by P-OH$\cdots NC_6H_5$ hydrogen bonding. Both phenomena should limit further protonation of the surface phosphate groups by solvating water. When considering the evolution of q_e with pH, it can be noticed that the amount of sorbed pyridine increases with pH over the whole range. In the low pH conditions where pyridinium ions are present, they cannot significantly interact with Ca^{2+} but may develop attractive electrostatic interactions with P-O^- groups. With increasing pH, the relative amount of pyridine over pyridinium increases that can more easily bind to the calcium ions. In the same time, P-OH$\cdots NC_6H_5$ hydrogen bonds may also arise, as mentioned above. In contrast, phenol sorption is more sensitive to the variation of the charge of the apatite surface and should therefore correspond to interactions with different chemical groups of the mineral surface, with the minimum sorption at pH 7-8 probably corresponding to the apatite pH point of zero charge (pH_{PZC}), in agreement with the literature [31,32]. Below pH_{PZC}, the overall apatite surface is positively charged and the oxygen atom of phenol may interact via Lewis acid-base interactions with Ca^{2+}. Above pH_{PZC}, the overall apatite surface charge is negative and hydroxyl groups of phenol may interact via hydrogen bonding with P-O^- moieties, as mentioned above. The possible modes of interaction of pyridinium, pyridine and phenol with the apatite surface have been gathered on Fig. 7. It is worth noting that Bronsted acid-base reaction between pyridine and P-OH may also occur but, because this occurs at the apatite surface, it is very likely that the resulting ionic pair P-O^-/C_6H_5N-H^+ remains associated, as in the case of direct pyridinium-phosphate interactions.

Another aspect to be discussed is related to surface coverage. Taking into account an average covering of 2 mg of pyridine per m^2 of apatite surface for PR, and assuming that the molecules will stand upright with their aromatic ring perpendicular to the mineral surface, it is possible to calculate that the sorption density is 1.5 pyridine molecule par nm^2, corresponding to a coverage of *ca.* 30% of the apatite surface. In parallel, the shortest Ca-Ca distance in the hydroxyapatite structure is reported to be *ca.* 0.35 nm [33], which is very close to the Van der Waals thickness of the pyridine ring. Thus, as already observed for TiO_2-rutile surface [34], it can be proposed that the pyridine rings are close-packed on the apatite surface, with aromatic rings parallel one with another. In contrast, for phenol, the surface coverage on PR is 0.25 mg per m^2. It can therefore be proposed that phenol adopt a titled configuration, as already observed on nickel oxide [35]. Coming back to pollutant chemical interactions with apatite surface, it is important to note that the upright position of pyridine is the most favorable for Lewis acid-base interactions between the nitrogen atom and the calcium ion whereas a titled configuration of phenol should provide a better conformation for hydrogen bond formation (Fig. 7).

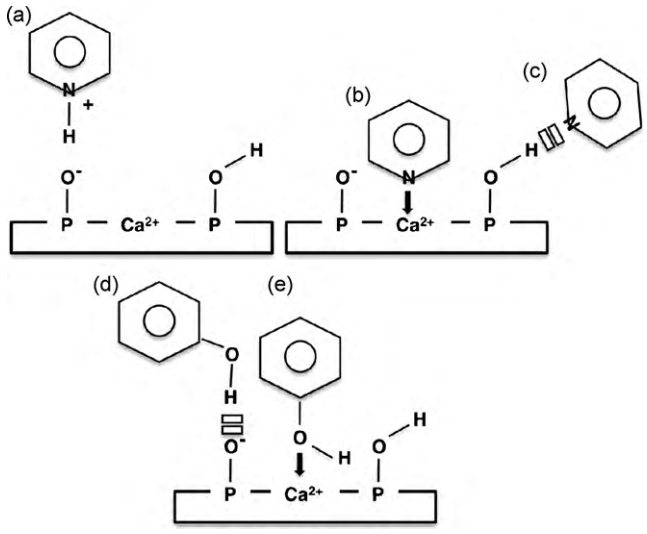

Fig. 7. Possible modes of interaction of (a) pyridinium, (b-c) pyridine and (d-e) phenol with apatite surface.

When coming to mesoporous materials, it is worth noting that the phenol sorption capacity does increase with the apatite specific surface area suggesting that the internal surface of mesopores is also accessible to this molecule. In contrast, the pyridine sorption capacity of c-HAp and p-HAp is not significantly different from that of PR. As pyridine size (*ca.* 0.65 nm along the main axis) is much smaller than the c-HAp and p-HAp average pore size (10 nm), its diffusion should be allowed in the porous structure of the apatite. Indeed, the mesopores correspond to voids between aggregated apatite particles. One possibility is therefore that pyridine sorption modifies particle aggregation and decreases the inter-particle pore size. Due to the low boiling point of pyridine (*ca.* 115 °C), it was not possible to analyze the porosity of the apatite materials after its sorption. However, attempts were made to put the pyridine-loaded apatite material in contact with phenol solution and it was found that, in this case, no phenol adsorption occurs, in agreement with our last hypothesis.

5. Conclusions

The results of this study show for the first time to our knowledge that natural apatite as well as synthetic apatites can efficiently be used for pyridine removal from aqueous media. Moreover, the natural phosphate shows pyridine sorption capacity as high as *ca.* 40 mgg^{-1}, being thus comparable with activated carbons that exhibit much higher specific surface area.[16] Therefore raw natural phosphate minerals that combine wide availability, limited environmental impact and low cost, can be used as such in remediation processes with a similar efficiency as treated waste materials, while avoiding heating/washing procedures [11,12]. It is now important to explore a much wider variety of organic pollutants to identify the full potentiality of apatite sorbents for specific waste removal. Particular attention will be paid to amine compounds whose toxicity is well-ascertained [36], and that are expected to exhibit a strong affinity for apatite surface, as suggested by the present study.

Acknowledgements

The authors would like to thank the “Office Chérifien des Phosphates (OCP)” and the “Centre d’Etudes et de Recherches des Phosphates Minéraux (CERPHOS) for their support.

References

[1] J.K. Fawell, S. Hunt, Environmental Toxicology: Organic Pollutants, Halstred Press, John Wiley and Sons, NY, 1998.
[2] Y.-M. Cho, U. Ghosh, A.J. Kennedy, A. Grossman, G. Ray, J.E. Tomaszewski, D.W. Smithenry, T.S. Bridges, R.G. Luthy, Field application of activated carbon amendment for in-situ stabilization of polychlorinated biphenyls in marine sediments, Environ. Sci. Technol. 43 (2009) 3815–3823.
[3] H.H. Fang, O. Chan, Toxicity of phenol towards anaerobic biogranules, Water Res. 31 (1997) 2229–2242.

[4] K.V. Padoley, S.N. Mudliar, R.A. Pandey, Heterocyclic nitrogenous pollutants in the environment and their treatment options—an overview, Bioresource Technol. 99 (2008) 4029–4043.
[5] J. Kaiser, Y. Feng, J.M. Bollag, Microbial metabolism of pyridine, quinoline, acridine and their derivatives under aerobic and anaerobic conditions, Microbiol, Rev. 60 (1996) 483–498.
[6] J. Li, W. Cai, J. Cai, The characteristics and mechanisms of pyridine biodegradation by *Streptomyces* sp, J. Hazard. Mater. 165 (2009) 950–954.
[7] H. Ucun, E. Yildiz, A. Nuhoglu, Phenol biodegradation in a batch jet loop bioreactor (JLB): Kinetics study and pH variation, Bioresource Technology 101 (2010) 2965–2971.
[8] S. Zhu, P.R.F. Bell, P.F. Greenfield, Adsorption of pyridine onto spent Rundle oil shale in dilute aqueous solution, Water Res. 22 (1988) 1331–1337.
[9] H. Bludau, H.G. Karge, W. Niessen, Sorption, sorption kinetics and diffusion of pyridine in zeolites, Microp, Mesop. Mater. 22 (1998) 297–308.
[10] D. Mohan, K.P. Sing, S. Sinha, D. Gosh, Removal of pyridine derivatives from aqueous solution by activated carbons developed from agricultural waste materials, Carbon 43 (2005) 1680–1693.
[11] P. Magne, P.L. Walker Jr., Phenol adsorption on activated carbons: application to the regeneration of activated carbons polluted with phenol, Carbon 24 (1986) 101–107.
[12] D. Mohan, K.P. Singh, S. Sinha, D. Gosh, Removal of pyridine from aqueous solution using low cost activated carbons derived from agricultural waste materials, Carbon 42 (2004) 2409–2421.
[13] J. Niu, B.E. Conway, Development of techniques for purification of waste waters: removal of pyridine from aqueous solution by adsorption at high-area C-cloth electrodes using in situ optical spectrometry, J. Electroanal. Chem. 521 (2002) 16–28.
[14] M. Stern, H. Elmar, O.M. Kut, K. Hungerbuhler, Removal of substituted pyridines by combined ozonation/fluidized bed biofilm treatment, Water Sci. Technol. 35 (1997) 329–335.
[15] S. Akita, H. Takeuchi, Sorption equilibria of pyridine derivatives in aqueous solution on porous resins and ion exchange resins, J. Chem. Eng. Jpn. 26 (1993) 237–241.
[16] S. Rengaraj, S.H. Moon, R. Sivabalan, B. Arabindoo, V. Murugesan, Removal of phenol from aqueous solution and resin manufacturing industry wastewater using an agricultural waste: rubber seed coat, J. Hazard. Mater. 89 (2002) 185–196.
[17] M. Mouflih, A. Aklil, S. Sebti, Removal of lead from aqueous solutions by activated phosphate, J. Hazard. Mater. 119 (2005) 183–188.
[18] S.B. Chen, Y.G. Zhu, Y.B. Ma, The effect of grain size of rock phosphate amendment on metal immobilization in contaminated soils, J. Hazard. Mater. 134 (2006) 74–79.
[19] A. Laghzizil, M. Mekkaoui, M. Ferhat, P. Barboux, Sorption of tribenuron-methyl onto apatite minerals, Toxicol. Environ. Chem. 81 (2001) 9–15.
[20] A. Bahdod, S. El Asri, A. Saoiabi, T. Coradin, A. Laghzizil, Adsorption of phenol from an aqueous solution by selected apatite adsorbents: kinetic process and impact of the surface properties, Water Res. 43 (2009) 313–318.
[21] K. Lin, J. Pan, Y. Chen, R. Cheng, X. Xu, Study of the adsorption of phenol from aqueous solution on apatite nanopowders, J. Hazard. Mater. 161 (2009) 231–240.
[22] S. El Asri, A. Laghzizil, A. Alaoui, A. Saoiabi, R. M'Hamdi, K. El Abbassi, A. Hakam, Structure and thermal behaviors of Moroccan phosphate rock (Bengurir), J. Therm. Anal. Calorim. 95 (2009) 15–19.
[23] S. El Asri, A. Laghzizil, A. Saoiabi, A. Alaoui, K. El Abassi, R. M'Hamdi, T. Coradin, A novel process for the fabrication of nanoporous apatites from Moroccan phosphate rock, Colloid Surf. A 350 (2009) 73–78.
[24] L. El Hammari, A. Laghzizil, P. Barboux, A. Saoiabi, K. Lahlil, Crystallinity and fluorine substitution effects on the proton conductivity of porous hydroxyapatites, J. Solid State Chem. 177 (2004) 134–138.
[25] L. El Hammari, A. Laghzizil, P. Barboux, K. Lahlil, A. Saoiabi, Retention of fluoride ions from aqueous solution using porous hydroxyapatite: Structure and conduction properties, J. Hazard. Mater. 114 (2004) 41–44.
[26] V. Srihari, A. Das, The kinetics and thermodynamic studies of phenol–sorption onto three agro-based carbons, Desalination 225 (2008) 220–234.
[27] Y.-S. Ho, Review of second-order models for adsorption systems, J. Hazard. Mater. 136 (2006) 681–689.
[28] H. Hu, M. Trejo, M.E. Nicho, J.M. Saniger, A. Garcia-Valenzuela, Adsorption kinetics of optochemical NH_3 gas sensing with semiconductor polyaniline films, Sensors Actuat. B 82 (2002) 14–23.
[29] Y. Otake, N. Kalili, T.H. Chang, E. Furuya, Relationship between Freundlich-type equation constants and molecular orbital properties, Separ. Purif. Technol. 39 (2004) 67–72.
[30] H. Tanaka, T. Watanabe, M. Chikazawa, FTIR and TPD studies on the adsorption of pyridine, n-butylamine and acetic acid on calcium hydroxyapatite, J. Chem. Soc., Faraday Trans. 93 (1997) 4377–4381.
[31] L.C. Bell, A.M. Posner, J.P. Quirk, The point of zero charge of hydroxyapatite and fluoroapatite in aqueous solutions, J. Colloid Interf. Sci. 42 (1973) 250–261.
[32] A. Bengtsson, A. Shchukarev, P. Persson, S. Sjöberg, A solubility and surface complexation study of a non-stoichiometric hydroxyapatite, Geochim. Cosmochim. Acta 73 (2009) 257–267.
[33] J.C. Elliot, Structure and Chemistry of the Apatites and other Calcium Orthophosphates, Elsevier, Amsterdam, 1994.
[34] B. Boddenberg, K. Eltzner, Adsorption and ^2H NMR of ammonia, pyridine, dimethylamine and benzene on rutile and anatase, Langmuir 7 (1991) 1498–1505.
[35] P. Kennedy, M. Petronio, H. Gisser, Competitive adsorption of phenol and sodium dinonylnaphtalenesulfonate on nickel oxide powder, J. Phys. Chem. 75 (1971) 1975–1980.
[36] G. Greenhouse, The evaluation of toxic effects of chemicals in fresh water using frog embryos and larvae, Environ. Poll. 11 (1970) 303–315.